Nanomed Res J 8(2):149-160, Spring 2023

RESEARCH ARTICLE

Pancreas recovery in diabetic rats after low dose curcumin@ZnO nanoparticles oral treatment

Gamal El-ghannam[1*], Eman I. Sobeh[2], Reda M. S. Korany[3], Hisham M. Saleh[2], Souad A Elfeky[1]

[1] National Institute of Laser Enhanced Sciences (NILES), Department of laser applications in Metrology, photochemistry, and agriculture, Cairo University, 12613, Giza, Egypt

[2] Biological Applications Department, Egyptian Atomic Energy Authority, Cairo, Egypt

[3] Pathology Department, Faculty of Veterinary Medicine, Cairo University, Cairo, Egypt

ARTICLE INFO

Article History:
Received 09 Jan 2023
Accepted 16 Apr 2023
Published 01 May 2023

Keywords:
Immunohistochemistry
CUR@ZnO NPs
Diabetes
Pancreas
Lesion

ABSTRACT

The purpose of this study was to explore the pancreas recovery in diabetic rats after treatment with the synthesized, curcumin@zinc oxide nanocomposite (CUR@ZnO NPs). Type 2 diabetes mellitus (T2DM) rats received low-dose treatments with Cur@ZnO NPs (1 mg/kg) for 4 weeks. The results indicated that CUR@ZnO NPs administration completely recovered T2DM rat's pancreas. Similarly, CUR@ZnO NPs were exceptional in improving the lipid profile of diabetic rats. The immunohistochemical investigation confirmed these results and revealed a complete recovery of pancreas and insulin production all over the pancreatic islets of the CUR@ZnO NPs group than in all other groups. Moreover, lesion scores in the pancreas and liver of T2DM rats given CUR@ZnO NPs showed a prodigious amelioration than the other groups. The previous results confirmed each other and indicate the success of CUR@ZnO NPs administration at low doses in the restoration of pancreas and insulin production in T2DM rats. The obtained results could help and guide the dose of CUR@ZnO NPs required as a novel drug for T2DM pancreas recovery.

How to cite this article
El-ghannam G., I. Sobeh E., M. S. Korany R., Saleh H. M., A Elfeky S. Pancreas recovery in diabetic rats after low dose curcumin@ZnO nanoparticles oral treatment. Nanomed Res J, 2023; 8(2): 149-160. DOI: 10.22034/nmrj.2023.02.004

INTRODUCTION

T2DM is a bundle of metabolic conditions that are identified by elevated blood glucose levels (hyperglycemia), insulin resistance (IR), and a relative deficiency in insulin [1]. This condition is considered one of the leading causes of mortality, ranking among the top five. Currently, diabetes affects over 150 million people worldwide, with projections indicating that this figure will double in the next two decades [2]. A significant proportion of T2DM patients are obese, which inherently contributes to some degree of insulin resistance (IR). Other individuals who are not overweight may exhibit a greater percentage of body fat, which can also lead to insulin resistance [3]. Extreme adiposity build-up is a known risk factor [3]. T2DM is linked with several metabolic and cardiovascular risk factors that lead to significant cardiovascular disease (CVD) and death rates [3].

Research in this area has been generally steered by the growing understanding of the contribution of metals to glucose metabolism and the link between metals deficiency and diabetes. Several metals, including Vanadium [4], Chromium [5], Magnesium [6], Cobalt [7], and Zinc [8] have been identified as having a role in glucose homeostasis and have been proposed as potential therapeutic agents for diabetes.

Zinc, an indispensable micronutrient, is linked to over 300 enzymes [9] and plays a significant role in a wide range of biological processes, including glucose metabolism. By influencing the insulin signaling pathway, zinc enhances hepatic glycogenesis, leading to improved utilization of glucose [10]. Additionally, it impedes the absorption of glucose in the intestines [11] and promotes glucose uptake in skeletal muscle and adipose tissue

* Corresponding Author Email: *g.ghanam@niles.cu.edu.eg*

[12]. Also, Zinc contributes to lowering circulating glucose levels and inhibits glucagon secretion [13], thus reducing gluconeogenesis.

Based on previous research, zinc is known to support the structural integrity of insulin [13] and is involved in insulin synthesis, storage, and secretion [6]. Zinc deficiency is linked to diabetes and can negatively impact the progression of T2DM [6]. The lack of zinc in the pancreas can reduce the production and release of insulin by β-cells, which is essential for maintaining glucose homeostasis [14]. Furthermore, zinc has antioxidant properties [6], and a decrease in zinc levels may worsen the complications of T2DM that result from oxidative stress. These observations highlight the complex relationship between zinc and diabetes. Developing zinc-based agents for treating T1DM, T2DM, and complications associated with both conditions is an attractive treatment strategy.

Studies conducted on diabetic rats have demonstrated the beneficial effects of zinc supplementation in diabetes management [15]. Synthesized zinc complexes have also proven effective in rodent models of diabetes [16]. Zinc oxide NPs are widely used in various products such as baby powder, barrier creams for diaper rash treatment, antidandruff shampoos, calamine cream, and antiseptic ointments [17, 18]. ZnO NPs surface capping is one of the valuable methods to overcome the aggregation of nanoparticles [19, 20].

Conversely, CUR has demonstrated significant effects on regulating blood glucose levels and stimulating gastric mucosal production in diabetic individuals [21]. Turmeric rhizomes have also exhibited antidiabetic properties, with the alcohol extract containing active ingredients that lower blood glucose levels in STZ-induced diabetic rats. However, CUR is mostly insoluble in water and has low bioavailability. [22]. To overcome this issue, nano-formulations of CUR can be developed to improve its stability and bioavailability. We aim to develop a potent novel CUR@ZnO NPs to restore the function of the pancreas in diabetic rats. Our study will investigate the immunohistochemical changes of the pancreas, blood glucose levels, lipid profile, and histopathological lesion scoring to evaluate the therapeutic potential of CUR@ZnO NPs in diabetic management.

MATERIALS AND METHODS

Preparation of ZnO NPs

To prepare the ZnO NPs, 2 grams of Zn $(CH_3COO)_2.2H_2O$ obtained from Sigma-Aldrich in the USA, was dissolved in 15 mL of distilled water. The solution was then stirred at 35°C for 20 minutes to obtain the zinc acetate solution. In a separate container, 8 grams of NaOH powder, also obtained from Sigma-Aldrich in the USA, was mixed with 10 milliliters of distilled water. The NaOH solution was also stirred at 35°C for approximately 20 minutes to dissolve the powder. The two solutions were then mixed, and 100 milliliters of ethanol was slowly added while vigorously stirring the mixture for about 90 minutes until a milky white solution was obtained. The solution was left to dry overnight at 80°C and subsequently calcined in an oven at 250°C for 4 hours to obtain the ZnO NPs. These methods for obtaining the ZnO NPs were adapted from previous research conducted in 2016 [23].

Preparation of CUR@ZnO NPs

To obtain the CUR@ZnO NPs, a stock solution of CUR obtained from Sigma-Aldrich in the USA was prepared in acetone with a concentration of 2 mg/mL (5.43 mmol). In parallel, 10 mg of ZnO NPs were dissolved in 1 mL of acetone, and the CUR solution was added to the ZnO solution. The resulting mixture was stirred for 24 hours to allow for granulation and surface adsorption of ZnO and CUR, resulting in the formation of CUR@ZnO nanoparticles. The suspension was then subjected to centrifugation at 6000 rpm, washed three times with distilled water, and dried under vacuum to obtain the final CUR@ZnO NPs [24].

Characterization of ZnO and CUR@ ZnO NPs

To analyze the morphology of the prepared ZnO and CUR@ZnO NPs, transmission electron microscopy (TEM) was utilized. TEM imaging was performed using a field-emission gun JEOL2010F transmission electron microscope operating at 120 kV. A diluted sample solution was deposited on an amorphous carbon-copper grid and left to evaporate at room temperature. Fourier transform infrared (FTIR) spectroscopy was utilized to determine the functional groups present in the synthesized CUR@ZnO NPs over a range of 4000-500 cm-1 using a Bruker Vertex 80 spectrometer. Absorption analysis was also conducted to assess the loading of CUR@ZnO NPs, with all spectra being obtained between 200-800 nm using a Perkin Elmer Lambda 40 spectrometer. The crystal structure of the CUR@ZnO was established through powder XRD analysis using the X-ray diffractometer

system X'Pert3 Powder from PANalytical in the Netherlands. The X-ray source was a Cu target (Cu Kα1), and measurements were conducted at room temperature with continuous scan type using settings of 30 kV and 30 mA. Particle size analysis was performed using Dynamic Light Scattering (DLS) measurement with a Malvern Zetasizer Nano ZS.

Animal experimental design

Biochemical experimental group design: Twenty male Wister rats, 2 months old, mean body weight of 150± 20 g were preserved according to the institutional animal care and use committee (CU-IACUC, Cairo University (CU-I-F-41-22), faculty of science, Cairo University-Egypt) (see supporting information). The control group (G1) was assigned as a reference, while the second group (G2) was given an oral dose of 1 mg/kg body weight of ZnO NPs [25]. The third group (G3) received an oral administration of 1 mg/kg body weight of curcumin-loaded zinc oxide nanoparticles (CUR@ ZnO NPs). The fourth group (G4) comprised of diabetic rats induced with STZ and did not receive any treatment. The fifth (G5) and sixth (G6) groups comprised STZ-induced diabetic rats, both of which were orally administered with a 1 mg/kg body weight dose of ZnO NPs and CUR@ZnO NPs, respectively, for a period of 30 days using a stomach tube.

T2DM induction in rats

Type 2 diabetes mellitus (T2DM) was induced in the rats by administering a single intraperitoneal injection of STZ (60 mg/kg), which was dissolved in a citrate solution with a pH of 4.5. After a fifteen-minute interval, nicotinamide (140 mg/ kg), dissolved in distilled water, was also injected intraperitoneally [26]. The rats were provided with a 5% glucose solution to drink overnight. The rats were considered diabetic when their blood glucose levels rose above 200 mg/dL on the third day following the STZ injection.

Immunohistochemistry

Immunohistochemical analysis was conducted using the methodology described by [27] (see supporting information).

Evaluation of insulin content in pancreatic islets

In each group, the quantitative immuno-reactivity was assessed in pancreatic islets [28]. Immuno-reactivity analysis was performed by examining 10 microscopic fields per section using a high-power microscope (400x magnification). The percentage of cells showing positive staining (%) was determined using the color deconvolution feature in ImageJ 1.52p software (developed by Wayne Rasband at the National Institutes of Health, U.S.A.).

Blood biochemical experiments

Blood samples were collected from the medial canthus of the eye under anesthesia in a dry and clean tube. For the determination of blood glucose levels, samples were collected after 10 days of treatment and at the end of the experiment.

Glucose

concentration was measured using the enzymatic colorimetric method with a commercial kit from Bio diagnostic and Research Reagent (Egypt), following the procedure described by Trinder in 1969 [29] (see supporting information).

Lipid profile

Cholesterol

concentration was determined using the enzymatic colorimetric method with a commercial kit from Bio diagnostic and Research Reagent (Egypt), following the procedure described in Richmond (1973) [30], [31] (see supporting information).

Triglyceride (TG)

concentration was measured using the enzymatic colorimetric method with a commercial kit from Bio diagnostic and Research Reagent (Egypt), following the procedure described by Fossati P and Prencipe L. in 1982 [32] (see supporting information).

HDL-Cholesterol (HDL-c)

concentration was determined using the enzymatic colorimetric method with a commercial kit from Bio diagnostic and Research Reagent (Egypt), following the procedure described by Burstein M. et al. in 1970 [33], [34] (see supporting information).

LDL-Cholesterol

concentration was assayed by the enzymatic colorimetric method using a commercial kit (Bio diagnostic and Research Reagent, Egypt) the

method described by H.Wieland and D. Seidel, 1983 [35], [36] (see supporting information).

Histopathological lesion scoring

At the conclusion of the experimental period, tissue samples were fixed in formalin and embedded in paraffin, then cut into 5-micron thick sections and stained with Hematoxylin and Eosin [37], [38] for histopathological examination and morphometric analysis (see supporting information). Histopathological changes in the pancreas and liver were assessed using a light microscope and scored as follows: no changes (0), mild changes (1), moderate changes (2), and severe changes (3). The scoring was determined based on the percentage of tissue showing alterations: <30% changes were considered mild, 30% to 50% changes were considered moderate, and >50% changes were considered severe [39, 40].

Statistical analysis

The data were presented as mean ± standard error (SE). Group differences were analyzed using one-way ANOVA, followed by Duncan's Multiple Range Test using SPSS version 21. A significance level of $P<0.05$ was used to determine statistical significance.

RESULTS AND DISCUSSION

Characterization of CUR@ZnO NPs

UV-Vis and FTIR

The optical absorbance of ZnO NPs is shown in **Fig. (1a)** at λ_{max} 360 nm, while that of CUR is at λ_{max} 425 nm. The absorbance of CUR@ZnO lies in between ZnO NPs and CUR at λ_{max} 370 nm. The shift of the absorption band of CUR@ZnO could be due to the capping of ZnO with CUR.

The loading amount of CUR @ the ZnO NPs was calculated according to Beer–Lambert law ($A = \varepsilon CL$) at λ_{max} 417 nm as indicated in Ref [41] (see supporting information). From Fig. (1b), the absorbance of the supernatant is 0.41 and its calculated concentration is $7.9*10^{-6}$ mol l^{-1}. The initial concentration was $1.6*10^{-5}$ mol l^{-1}. Thus, the amount of CUR loaded in the nano-composite system is $8.1*10^{-6}$ mol l^{-1}.

The FTIR spectra of ZnO NPs, CUR, and CUR@ZnO NPs exhibit a broad peak in the range of 3600 to 3050 cm^{-1}, which corresponds to the stretching vibration of the hydroxyl (OH) group (Fig. 1c). The IR peaks of ZnO are observed at 520, 910, 1381, and 1548 cm^{-1}, as previously reported [42]. The peak at 2932 cm^{-1} corresponds to the aromatic C-H stretch vibrations, while the band at 1636 cm^{-1} is attributed to the C=O stretching of CUR, as described in [43]. Additionally, the C-O-C stretching vibrations are observed at 1024 cm^{-1}. In the FTIR spectra of CUR@ZnO NPs, the presence of Zn-O bands at 520, 910, and 1381 cm^{-1}, along with the CUR bands showing slight shifts, confirms the capping of ZnO NPs with CUR.3.1.2. XRD and TEM.

The XRD of ZnO NPs in **Fig. (2a)** displays peaks at 2θ 31.64°, 34.85°, 36.65°, 46.1°, 57.12°, 63.2°, and 68.9° which correspond to the (100), (002), (101) (102) (110), (103) and (112) planes of the hexagonal crystal phase (JCPDF No. 36-1451) [44].

The average size of the crystal (24±5 nm) was anticipated by using the Scherrer formula [45], using the diffraction intensity of (101) peak. The capping of CUR@ ZnO did not affect the crystal planes, as seen from the XRD of CUR@ZnO NPs.

Characterization of ZnO NPs was also performed by TEM to verify the shape and particle size of Fig. (2b). TEM image show a spherical shape of ZnO NPs with a mean size of about 30±5 nm for ZnO NPs.

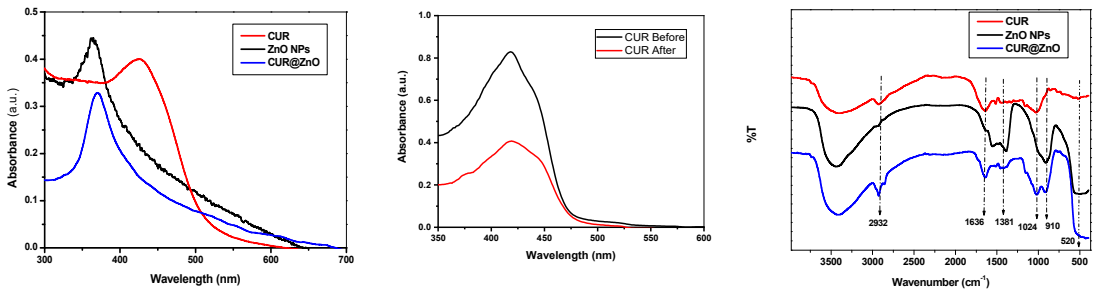

Fig. 1. (a) Optical absorbance of ZnO NPs, CUR, and CUR@ZnO NPs, (b) optical absorbance of CUR at initial concentration (CUR before) and the unreacted CUR (CUR after) in the supernatant after nanocomposite formation, and (c) FTIR spectrum of ZnO NPs, CUR, and CUR@ZnO NPs.

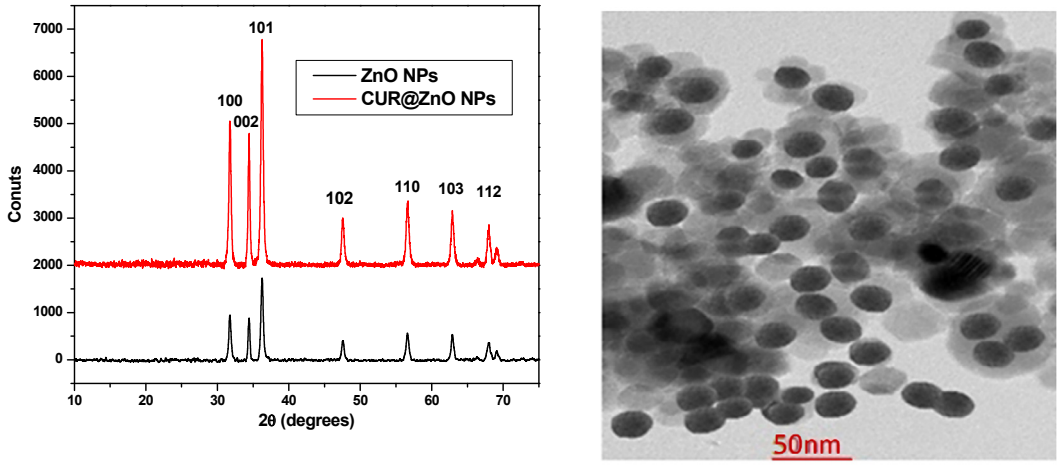

Fig. 2. (a) XRD Pattern of ZnO NPs, (b). TEM image of ZnO NPs

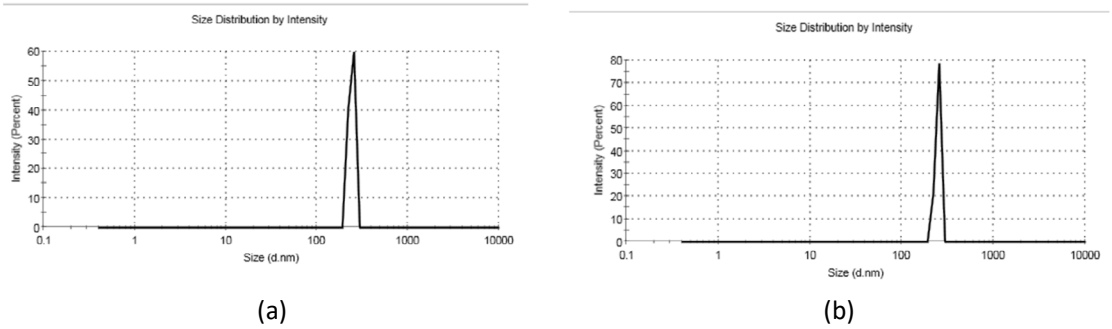

Fig. 3. The hydrodynamic diameter (d.nm) of ZnO and CUR@ZnO NPs based on the diffusion of the particles using DLS analysis.

DLS analysis

Fig. (3) showed the distribution profile of ZnO NPs, and CUR@ZnO NPs via DLS measurement. The maximum intensity is at 241 and 247.5 nm for ZnO NPs, and CUR@ZnO NPs respectively. Comparable results were obtained by [46] for ZnO Nps (223 nm). They found that the increase in the size distribution profile of NPs is due to the low viscosity of water, resulting in high agglomeration as compared to other solvents like ethylene glycol.

Immunohistochemical analysis of pancreas recovery and insulin expression in diabetic rats

The control group, the group treated with ZnO NPs and the group treated with CUR@ZnO NPs showed a wide range of insulin resistance in all pancreatic islets (positive anti-insulin immunostaining) (Figs. 4a, b, and c). In contrast, the STZ-treated group showed a significant decrease in β-cells insulin content (Fig. 4d). The group treated with STZ followed by ZnO NPs revealed a slight enhancement of the insulin content related to the STZ-treated group (Fig. 4e). However, the group treated with STZ followed by CUR@ZnO NPs exhibited a progressive improve in the insulin content of β-cells, reaching levels similar to the untreated control group (Fig. 4f). The percentage area ± SE of anti-insulin immunostaining in β-cells for the different treated groups is depicted in Fig. 4g.

Concerning the group treated with STZ then ZnO NPs there was a mild improvement in both histopathological alteration and insulin content of β-cells, while the group treated with STZ then CUR@ZnO NPs showed obvious amelioration in the aforementioned symptoms. It is known that ZnO NPs are antidiabetic agents [47] by enhancing the release of insulin in rat pancreatic islets in response to glucose. In addition, natural plants with antioxidant properties and their main

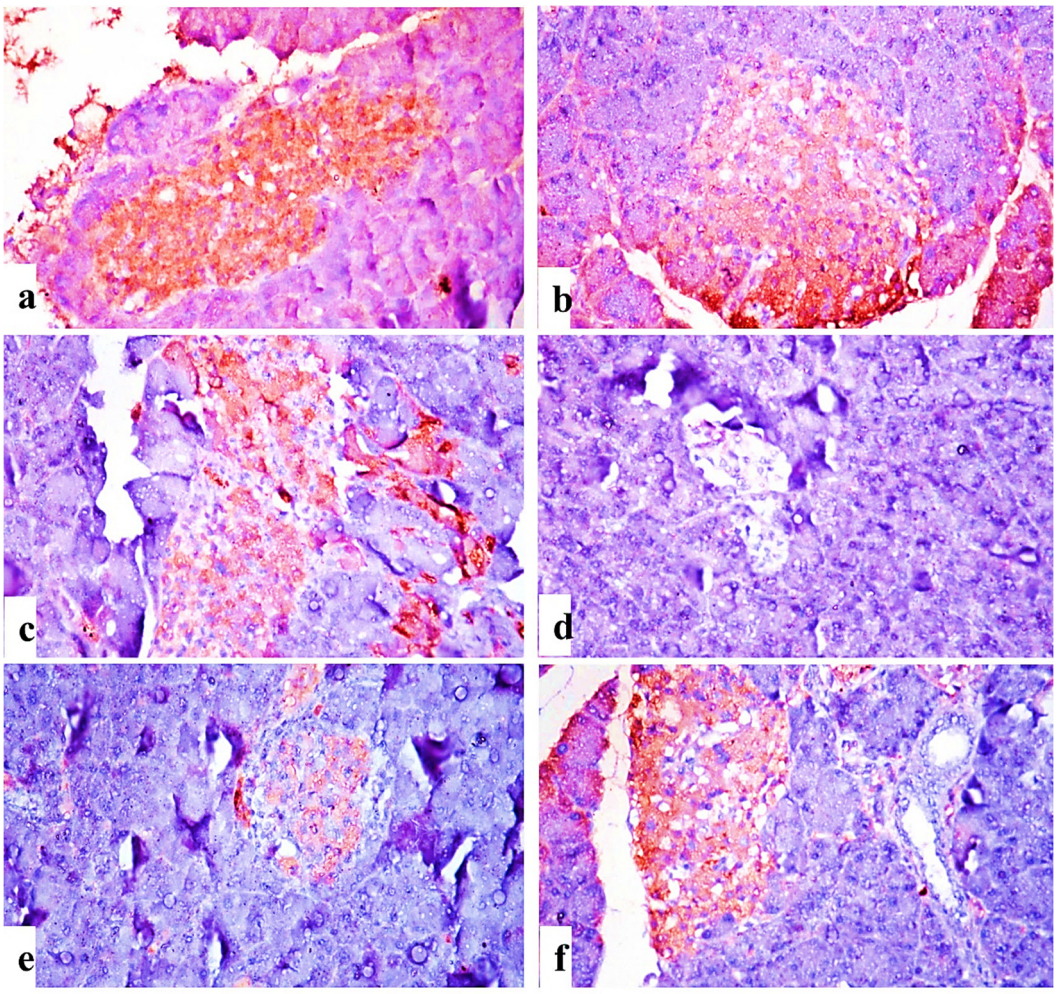

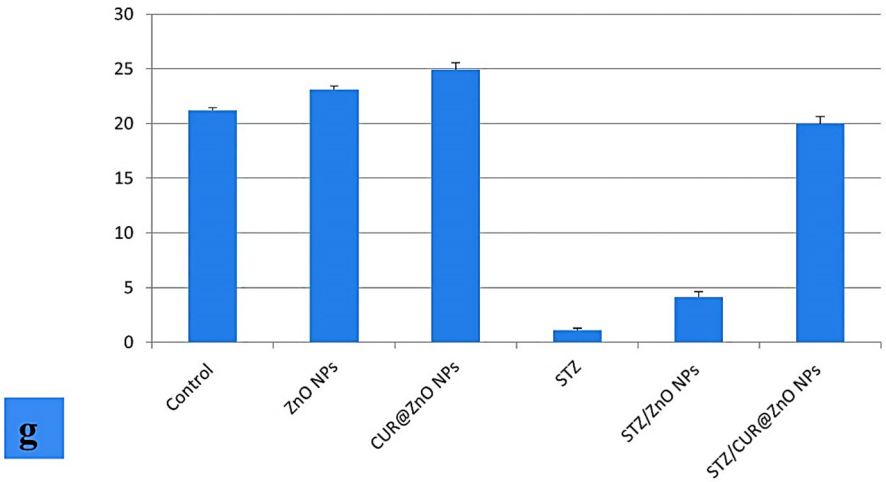

Fig. 4. Immunohistochemical staining of anti-insulin in the pancreas. (a), (b), and (c) are the control, ZnO NPs, and CUR@ZnO NPs treated groups respectively. (d) STZ treated group, (e) group treated with STZ and ZnO NPs. (f) the group treated with STZ and CUR@ ZnO NPs, (g) immunostaining expression of anti-insulin % area ± SE in β-cells of different treated groups (Anti-insulin H&EX400), P value ≥0.05.

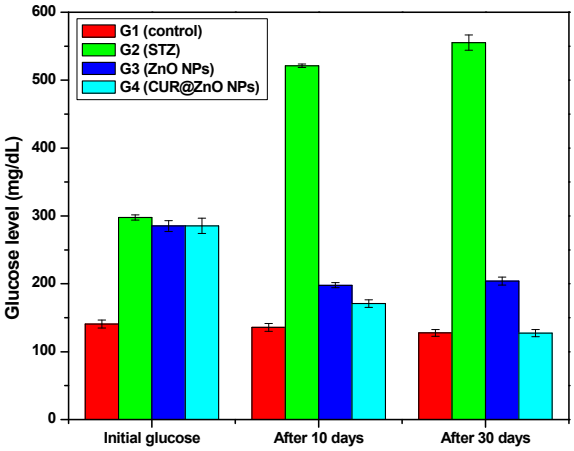

Groups	Initial glucose (mg/dL)	After 10 days (mg/dL)	Final glucose(mg/dL)
Control (G1)	140.8^{a}±5.9	135.8 ^{a}±5.7	127.8^{a}± 4.9
STZ (G2)	297.76^{b}± 3.9	521.2 ^{c}± 2.4	555.2^{c}±11.3
STZ/ZnO NPs (G3)	285.2^{b}±8	197.9 ^{b}±3.7	204^{b}± 5.9
STZ/CUR@ZnO NPs (G4)	285.3^{b}± 11.3	170.9^{a} ± 5.6	127.4^{a}±5.2

Fig. 5. Effects of ZnO NPs and CUR@ZnO NPs on blood glucose level of STZ-diabetic-rats.
Data are presented as change ± S.E, S.E. Standard Error (means within the same columns carrying different superscripts are significantly different at $p<0.05$).

products are considered useful in the treatment of diabetes because they prevent oxidative stress caused by hyperglycemia and have beneficial effects on glucose metabolism [48]. Thus CUR@ZnO NPs treatment revealed a strong indication of pancreatic islet renewal in diabetic rats. Abdel Aziz et al. 2013 [49] had similar results when treating rats with CUR derivatives for 40 days. This may be linked to the anti-inflammatory and antioxidant properties of curcumin [50], and support of the immune system and pancreatic cells for islet regeneration. The effects of curcumin on cell growth and stem cell differentiation may also be implicated.

Biochemical analysis

Effect of CUR@ZnO NPs on the blood glucose level of rats

T2DM syndromes rely on insulin resistance, chronic hyperglycemia, and variation in protein, lipid, and carbohydrate metabolism [51]. It can also occur when the insulin receptors block the action of insulin. The reported enhanced role of ZnO or CUR in T2DM pathogenesis, in particular through its effect on insulin synthesis [15, 52] makes the orally administered CUR@ZnO NPs a promising T2DM therapeutic agent due to the easy passage through the biological membranes [14, 53]. The effects of ZnO NPs and CUR@ZnO NPs on blood glucose concentration of STZ-diabetic-rats is shown in **Fig. (5)**.

Following STZ administration, blood glucose levels in untreated diabetic rats (G2) remained constant over the study period. These levels were significantly higher ($p< 0.05$) compared to the nondiabetic control group (G1). However, the administration of ZnO NPs (G3) and CUR@ZnO NPs (G4) effectively reduced the elevated glucose levels in diabetic rats. Notably, treatment with CUR@ZnO NPs normalized the glucose levels to values comparable to the control group. The increase in blood glucose in diabetic rats is due to STZ-induced destruction of pancreatic β-cells, which leads to production of reactive oxygen species and oxidative stress. Furthermore, STZ may cause damage to the DNA of pancreatic islet cells. Previous studies have indicated that zinc enhances insulin release in response to glucose in isolated rat pancreatic islets [52]. CUR may also contain chemicals capable of modifying or stimulating insulin receptors, altering the structure

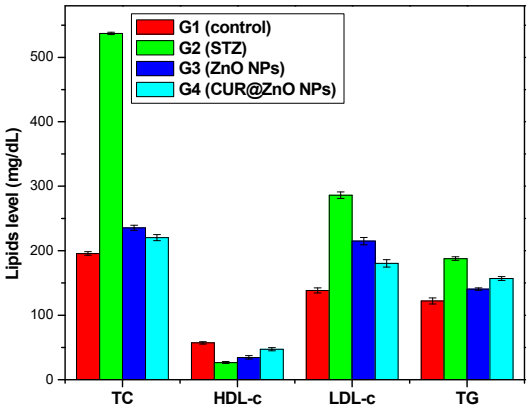

Groups	TC (mg/dL)	HDL-c (mg/dL)	LDL-c(mg/dL)	TG (mg/dL)
Control (G1)	195.66[a]± 2.68	57.21 [c] ± 4.48	138.44 [a] ± 4.08	122.33[a]±3.24d
STZ (G2)	537[c]± 1.77	26.71 [a] ± 1.54	286.20 [d] ± 5.16	187.87[d]± 2.81a
STZ/ZnO NPs (G3)	235.66 [b] ± 3.99	34.66 [a] ± 2.6	214.92 [c] ± 5.66	140.56[b]± 1.99c
STZ/CUR@ZnO NPs (G4)	220.25 [b] ± 4.75	47.25 [b] ± 2.3	180.43 [b] ±5.68	156.89c± 2.90 b

Fig. 6. The effect of ZnO NPs and CUR@ZnO NPs on the lipid profile of STZ-diabetic rats.
Data are presented as change ± S.E, S.E. Standard Error (means within the same columns carrying different superscripts are significantly different at $p<0.05$).

of glucose transport proteins, and suppress insulin antagonists in the body [51]. The obtained standard error (S.E.) values support these interpretations of the data. There is evident variation in the S.E. values among the initial glucose-treated groups (G2, G3, G4) compared to the control group (G1). However, this variation tends to decrease after treatments, especially with STZ/CUR@ZnO NPs (G4) and then STZ/ZnO NPs (G3). On the other hand, the S.E. values for the STZ group (G2) continue to increase due to uncontrolled blood glucose levels. Statistical analysis reveals that means with different superscripts within the same column are significantly different at $p<0.05$.

Effect of CUR@ZnO NPs on lipid profile parameters of rats

As known, a chronic diabetic state is associated with dyslipidemia. STZ-treated rats (G2) showed higher total cholesterol (TC), Triglycerides (TG), LDL-c, and a significantly lower HDL-c when compared with the other groups (**Fig. 6**). Similar results were obtained by Umrani and Paknikar. 2014 [47].

In contrast, ZnO NPs and CUR@ZnO NPs treated groups (G3 and G4) exerted a significant decrease in TG, TC, and LDL-c and a marked increase in HDL-c compared to STZ-diabetic rats (G2). But, CUR@ZnO NPs evoked better results compared to ZnO NPs treated rats. Previous studies revealed the role of dietary CUR in lowering diabetic rats' cholesterol through stimulation of hepatic cholesterol-7a-hydroxylase [53]. In addition, CUR lowers LDL in diabetic rats by increasing hepatic LDL receptor number through stimulation of HMG-CoA reductase activity [54]. However, it was reported that dietary CUR lowers the lipoprotein lipase enzyme which regulates the triglycerides level in rats [55]. Thus, TG in G4 is higher than that of G3. The increase in the HDL-C level in diabetic rats treated with CUR@ZnO may be due to the reduction of LDL-C and the role of CUR in activating the Lpl enzyme and enhancing insulin to hydrolyze triglycerides [56]. Similarly, ZnO NPs enhance the release of insulin in diabetic rat pancreas. Consequently, CUR@ZnO exerted a higher effect than ZnO NPs in improving the diabetic rats' lipid profile. The S.E. rate of the rat's lipid profile among the control (G1) and STZ-treated groups (G2, G3, G4) showed variability

Table 1. Scoring of histopathological lesions in pancreas and liver of all treated groups

Lesions	Control (G1)	ZnO NPs (G2)	CUR@ZnO NPs (G3)	STZ (G4)	STZ/ZnO NPs (G5)	STZ/CUR@ ZnO NPs (G6)
pancreas:						
- Atrophy and distortion of islets of Langerhans	0	0	0	3	2	0
- Vacuolar degeneration of exocrine pancreas	0	0	0	3	2	1
- Congestion of interstitial blood vessels	0	0	0	2	1	0
- Peri-ductal fibrosis of exocrine pancreas.	0	0	0	3	2	1
Liver:						
- Vacuolar degeneration and necrosis of hepatocytes	0	0	0	2	1	0
- Congestion of central veins and blood sinusoids	0	0	0	3	2	1
- Portal edema, congestion	0	0	0	3	2	1
- Portal mononuclear inflammatory cells infiltration	0	0	0	2	1	0
- Bile duct hyperplasia	0	0	0	2	1	1

in the sampling distribution of means. While means within the same columns carrying different superscripts are significantly different at $p<0.05$.

Histopathological lesion scoring of pancreas and liver

All lesions in the pancreas and liver were assessed based on their severity (see supporting information of histopathological findings of pancreas and liver in Figs. S1 and S2 respectively) as shown in Table (1). The scoring method was formulated as follows: score 0 = absence of the lesion in all rats of the group (n= 5), score 1= (<30%), score 2= (<30% – 50%), and score 3= (>50%) [39,40].

Pancreas

The pancreas of control, ZnO NPs, and CUR@ ZnO NPs treated groups showed no lesion scoring as shown in the histological structure of Langerhans islets and exocrine pancreas (**Fig**. S1 a-c). This means that ZnO NPs, and CUR@ZnO NPs are safe for application in insulin and pancreas recovery in diabetic patients. The STZ treated group showed the highest lesion scoring 3 due to atrophy and distortion of islets of Langerhans islets, peri-ductal fibrosis of exocrine pancreas, and hyperplasia of the ductal epithelium (**Fig**. S1 e-h) [57]. The STZ-induced diabetic group treated with ZnO NPs showed moderate lesion scoring due to restoration of the size of islets of Langerhans with moderate vacuolation of the exocrine pancreas (**Fig**. S1 i). The STZ-induced diabetic group treated with CUR@ ZnO NPs showed zero to 1 lesion scoring as the Langerhans islets and exocrine pancreas recovered and became nearly normal (**Fig**. S1 j).

Liver: The control, ZnO NPs, and CUR@ZnO NPs treated groups has no lesion scoring as revealed by the normal histological liver structure (**Fig.** S2 a-c). In the STZ treated group, the lesion scoring was 2-3 as hepatocytes revealed the presence of vacuolar degeneration and necrosis with congestion of central veins and blood sinusoids as well as hyperplasia of bile ducts with infiltration of a few mononuclear inflammatory cells (**Fig**.S2 d-g) [58,61]. The group treated with STZ and then ZnO NPs showed mild improvement of the previously mentioned lesions (**Fig.** S2 h). The group treated with STZ then CUR@ZnO NPs confirmed the minimum lesion score Zero-1 due to great recovery of hepatocytes and central vein (**Fig.** S2 i).

CONCLUSION

ZnO NPs were synthesized by the chemical reduction method. CUR was then loaded on ZnO NPs until complete granulation/surface adsorption of CUR@ZnO. TEM, XRD, FTIR, and UV-Vis verified the formation of hexagonal ZnO NPs nanocrystals and the loading of CUR@ZnO NPs. The immunohistochemical study disclosed that ZnO NPs are antidiabetic agents by enhancing the release of insulin in rat pancreatic islets in response to glucose. However, CUR@ZnO NPs treatment revealed a strong indication of pancreatic islet renewal in diabetic rats. Biochemical analysis illustrated that both ZnO NPs and CUR@ZnO NPs reduced the blood glucose of the diabetic rats, but CUR@ZnO NPs treatment rendered the glucose level to the normal control value after 30 days of treatment (1 mg/kg). Similarly, CUR@ ZnO NPs exerted a significant decrease in TG, TC, and LDL-c and a marked increase in HDL-c more than ZnO-NPs in treated diabetic rats. The histopathological lesion scoring of the pancreas and

liver of diabetic rats showed a better recovery in the case of CUR@ZnO NPs treatment than ZnO NPs and confirmed the obtained immunohistochemical and biochemical results. Thus, the best retrieval of diabetic symptoms was obtained with CUR@ZnO NPs treatment at a dose of 1 mg/kg for 30 days. This recommended dose could lead to the production of an oral drug for permanent diabetic recovery.

ACKNOWLEDGEMENT

We would like to acknowledge the support provided by the National Institute of Laser Enhanced Sciences (NILES), Cairo University, Egypt, the Atomic Energy Authority, Egypt, and the Faculty of Veterinary Medicine, Cairo University, Egypt, for their contribution to this work.

FUND

However, it is important to note that this research did not receive any specific grant from funding agencies in the public, commercial, or not-for-profit sectors.

AUTHOR CONTRIBUTION

Souad A Elfeky and Gamal El-ghannam prepared and characterized the ZnO/CUR NC. Eman I. Sobeh, and H. M. Saleh, animal breeding, feeding, treatment and sacrifice animals. Reda M. S. Korany Immunohistological studies and lesion scoring.

CONFLICT OF INTEREST

The authors have no conflict of interest to declare.

REFERENCES

1. R. A. Mohamed, O. Galal, A. R. Mohammed, and H. S. El-Abhar, Tropisetron modulates peripheral and central serotonin/insulin levels via insulin and nuclear factor kappa B/receptor for advanced glycation end products signalling to regulate type-2 diabetes in rats, RSC advances, vol. 8, pp. 11908-11920, 2018. https://doi.org/10.1039/C7RA13105D
2. Y. Lin and Z. Sun, Current views on type 2 diabetes, The Journal of endocrinology, vol. 204, p. 1, 2010. https://doi.org/10.1677/JOE-09-0260
3. M. A. Kamal, M. H. Khairy, N. A. ELSadek, and M. Hussein, Therapeutic efficacy of zinc oxide nanoparticles in diabetic rats, Slovenian Veterinary Research, vol. 56, 2019. https://doi.org/10.26873/SVR-756-2019
4. K. H. Thompson, J. Lichter, C. LeBel, M. C. Scaife, J. H. McNeill, and C. Orvig, Vanadium treatment of type 2 diabetes: a view to the future, Journal of inorganic biochemistry, vol. 103, pp. 554-558, 2009. https://doi.org/10.1016/j.jinorgbio.2008.12.003
5. Z. Q. Wang and W. T. Cefalu, Current concepts about chromium supplementation in type 2 diabetes and insulin resistance, Current diabetes reports, vol. 10, pp. 145-151, 2010. https://doi.org/10.1007/s11892-010-0097-3
6. I. C. Wells, Evidence that the etiology of the syndrome containing type 2 diabetes mellitus results from abnormal magnesium metabolism, Canadian journal of physiology and pharmacology, vol. 86, pp. 16-24, 2008. https://doi.org/10.1139/Y07-122
7. H. Vasudevan and J. H. McNeill, Chronic cobalt treatment decreases hyperglycemia in streptozotocin-diabetic rats, Biometals, vol. 20, pp. 129-134, 2007. https://doi.org/10.1007/s10534-006-9020-4
8. A. B. Chausmer, Zinc, insulin and diabetes, Journal of the American College of Nutrition, vol. 17, pp. 109-115, 1998. https://doi.org/10.1080/07315724.1998.10718735
9. J. Jansen, W. Karges, and L. Rink, Zinc and diabetes-clinical links and molecular mechanisms, The Journal of nutritional biochemistry, vol. 20, pp. 399-417, 2009. https://doi.org/10.1016/j.jnutbio.2009.01.009
10. E. Ueda, Y. Yoshikawa, H. Sakurai, Y. Kojima, and N. M. Kajiwara, In vitro alpha-glucosidase inhibitory effect of Zn (II) complex with 6-methyl-2-picolinmethylamide, Chemical and pharmaceutical bulletin, vol. 53, pp. 451-452, 2005. https://doi.org/10.1248/cpb.53.451
11. H. Ishihara, P. Maechler, A. Gjinovci, P.-L. Herrera, and C. B. Wollheim, Islet β-cell secretion determines glucagon release from neighbouring α-cells, Nature cell biology, vol. 5, pp. 330-335, 2003. https://doi.org/10.1038/ncb951
12. L. Egefjord, A. B. Petersen, A. M. Bak, and J. Rungby, Zinc, alpha cells and glucagon secretion, Current diabetes reviews, vol. 6, pp. 52-57, 2010. https://doi.org/10.2174/157339910790442655
13. Q. Sun, R. M. Van Dam, W. C. Willett, and F. B. Hu, Prospective study of zinc intake and risk of type 2 diabetes in women, Diabetes care, vol. 32, pp. 629-634, 2009. https://doi.org/10.2337/dc08-1913
14. J. A. Meyer and D. M. Spence, A perspective on the role of metals in diabetes: past findings and possible future directions, Metallomics, vol. 1, pp. 32-41, 2009. https://doi.org/10.1039/B817203J
15. J. Uyoyo Ukperoro, N. Offiah, T. Idris, and D. Awogoke, Antioxidant effect of zinc, selenium and their combination on the liver and kidney of alloxan-induced diabetes in rats, Mediterranean Journal of Nutrition and Metabolism, vol. 3, pp. 25-30, 2010. https://doi.org/10.1007/s12349-009-0069-9
16. S. Karmaker, T. K. Saha, Y. Yoshikawa, and H. Sakurai, A zinc (II)/poly (γ-glutamic acid) complex as an oral therapeutic for the treatment of type-2 diabetic KKAy mice, Macromolecular bioscience, vol. 9, pp. 279-286, 2009. https://doi.org/10.1002/mabi.200800190
17. O. Akhavan and E. Ghaderi, Enhancement of antibacterial properties of Ag nanorods by electric field, Science and technology of advanced materials, 2009. https://doi.org/10.1088/1468-6996/10/1/015003
18. F. Harding, Breast cancer: cause, prevention, cure: Tekline publishing, 2006.
19. F. Yuan, H. Peng, Y. Yin, Y. Chunlei, and H. Ryu, Preparation of zinc oxide nanoparticles coated with homogeneous Al2O3 layer, Materials Science and Engineering: B, vol. 122, pp. 55-60, 2005. https://doi.org/10.1016/j.mseb.2005.04.016
20. N. El-Kattan, A. N. Emam, A. S. Mansour, M. A. Ibrahim, A. B. Abd El-Razik, K. A. Allam, et al., Curcumin assisted green synthesis of silver and zinc oxide nanostructures and their antibacterial activity against some clinical pathogenic multi-drug resistant bacteria, RSC advances, vol. 12, pp.

18022-18038, 2022. https://doi.org/10.1039/D2RA00231K
21. H. Nasri, N. Sahinfard, M. Rafieian, S. Rafieian, M. Shirzad, and M. Rafieian-Kopaei, Turmeric: A spice with multifunctional medicinal properties, Journal of HerbMed Pharmacology, vol. 3, 2014.
22. M. Modasiya and V. Patel, Studies on solubility of curcumin, Int. J. Pharm. Life Sci, vol. 3, pp. 1490-1497, 2012.
23. D. Cao, S. Gong, X. Shu, D. Zhu, and S. Liang, Preparation of ZnO nanoparticles with high dispersibility based on oriented attachment (OA) process, Nanoscale research letters, vol. 14, pp. 1-11, 2019. https://doi.org/10.1186/s11671-019-3038-3
24. W. Perera, R. K. Dissanayake, U. Ranatunga, N. Hettiarachchi, K. Perera, J. M. Unagolla, et al., Curcumin loaded zinc oxide nanoparticles for activity-enhanced antibacterial and anticancer applications, RSC advances, vol. 10, pp. 30785-30795, 2020. https://doi.org/10.1039/D0RA05755J
25. S. Asri-Rezaei, B. Dalir-Naghadeh, A. Nazarizadeh, and Z. Noori-Sabzikar, Comparative study of cardio-protective effects of zinc oxide nanoparticles and zinc sulfate in streptozotocin-induced diabetic rats, Journal of Trace Elements in Medicine and Biology, vol. 42, pp. 129-141, 2017. https://doi.org/10.1016/j.jtemb.2017.04.013
26. T. Szkudelski, Streptozotocin-nicotinamide-induced diabetes in the rat. Characteristics of the experimental model, Experimental biology and medicine, vol. 237, pp. 481-490, 2012. https://doi.org/10.1258/ebm.2012.011372
27. R. A. Azouz and R. Korany, Toxic impacts of amorphous silica nanoparticles on liver and kidney of male adult rats: an in vivo study, Biological Trace Element Research, vol. 199, pp. 2653-2662, 2021. https://doi.org/10.1007/s12011-020-02386-3
28. N. Saleh, T. Allam, R. M. Korany, A. M. Abdelfattah, A. M. Omran, M. A. Abd Eldaim, et al., Protective and therapeutic efficacy of hesperidin versus cisplatin against Ehrlich ascites carcinoma-induced renal damage in mice, Pharmaceuticals, vol. 15, p. 294, 2022. https://doi.org/10.3390/ph15030294
29. P. Trinder, Determination of glucose in blood using glucose oxidase with an alternative oxygen acceptor, Annals of clinical Biochemistry, vol. 6, pp. 24-27, 1969. https://doi.org/10.1177/000456326900600108
30. W. Richmond, Preparation and properties of a cholesterol oxidase from Nocardia sp. and its application to the enzymatic assay of total cholesterol in serum, Clinical chemistry, vol. 19, pp. 1350-1356, 1973. https://doi.org/10.1093/clinchem/19.12.1350
31. C. C. Allain, L. S. Poon, C. S. Chan, W. Richmond, and P. C. Fu, Enzymatic determination of total serum cholesterol, Clinical chemistry, vol. 20, pp. 470-475, 1974. https://doi.org/10.1093/clinchem/20.4.470
32. P. Fossati and L. Prencipe, Serum triglycerides determined colorimetrically with an enzyme that produces hydrogen peroxide, Clinical chemistry, vol. 28, pp. 2077-2080, 1982. https://doi.org/10.1093/clinchem/28.10.2077
33. M. Burstein, H. Scholnick, and R. Morfin, Rapid method for the isolation of lipoproteins from human serum by precipitation with polyanions, Journal of lipid research, vol. 11, pp. 583-595, 1970. https://doi.org/10.1016/S0022-2275(20)42943-8
34. M. F. Lopes-Virella, P. Stone, S. Ellis, and J. A. Colwell, Cholesterol determination in high-density lipoproteins separated by three different methods, Clinical chemistry, vol. 23, pp. 882-884, 1977. https://doi.org/10.1093/clinchem/23.5.882
35. H. Wieland and D. Seidel, A simple specific method for precipitation of low density lipoproteins, Journal of lipid research, vol. 24, pp. 904-909, 1983. https://doi.org/10.1016/S0022-2275(20)37936-0
36. Reitman and S. Frankel, A colorimetric method for the determination of serum glutamic oxalacetic and glutamic pyruvic transaminases, American journal of clinical pathology, vol. 28, pp. 56-63, 1957. https://doi.org/10.1093/ajcp/28.1.56
37. J. D. Bancroft and M. Gamble, Theory and practice of histological techniques: Elsevier health sciences, 2008.
38. C. Ricordi and C. Rastellini, In Ricordi C (ed): Methods in Cell Transplantation, Austin, Tex: Landes, 1995.
39. R. M. Korany, K. S. Ahmed, H. Halawany, and K. A. Ahmed, Effect of long-term arsenic exposure on female Albino rats with special reference to the protective role of Spirulina platensis, Explor Anim Med Res, vol. 9, pp. 125-136, 2019.
40. D. A. Madkour, M. M. Ahmed, S. H. Orabi, S. M. Sayed, R. M. Korany, and H. K. Khalifa, Nigella sativa oil protects against emamectin benzoate-Induced neurotoxicity in rats, Environmental Toxicology, vol. 36, pp. 1521-1535, 2021. https://doi.org/10.1002/tox.23149
41 R. M. Amin, S. A. Elfeky, T. Verwanger, B. Krammer, A new biocompatible nanocomposite as a promising constituent of sunscreens, Mater Sci Eng C Mater Biol Appl,. 2016 vol. 63, pp. 46-51, 2016. https://doi.org/10.1016/j.msec.2016.02.044
42. M. H. H. Chai, N. Amir, N. Yahya, and I. M. Saaid, Characterization and colloidal stability of surface modified zinc oxide nanoparticle, in Journal of Physics: Conference Series, 2018, p. 012007. https://doi.org/10.1088/1742-6596/1123/1/012007
43. T. M. S. U. Gunathilake, Y. C. Ching, H. Uyama, N. D. Hai, and C. H. Chuah, Enhanced curcumin loaded nanocellulose: a possible inhalable nanotherapeutic to treat COVID-19, Cellulose, vol. 29, pp. 1821-1840, 2022. https://doi.org/10.1007/s10570-021-04391-8
44. S. A. Elfeky and S. M. Reda, MOF/Up-converting combination for photovoltaic application, Journal of Electroanalytical Chemistry, vol. 895, p. 115485, 2021. https://doi.org/10.1016/j.jelechem.2021.115485
45. S. A., S. E. Mahmoud, and A. F. Youssef, Applications of CTAB modified magnetic nanoparticles for removal of chromium (VI) from contaminated water, Journal of advanced research, vol. 8, pp. 435-443, 2017. https://doi.org/10.1016/j.jare.2017.06.002
46. M. Kasahun, A. Yadate, A. Belay, Z. Belay, M. Ramalingam, Antimicrobial Activity of Chemical, Thermal and Green Route-Derived Zinc Oxide Nanoparticles: A Comparative Analysis, Nano Biomed. Eng, Vol. 12, Iss. 1, 2020. https://doi.org/10.5101/nbe.v12i1.p47-56
47. R. D. Umrani and K. M. Paknikar, Zinc oxide nanoparticles show antidiabetic activity in streptozotocin-induced Type 1 and 2 diabetic rats, Nanomedicine, vol. 9, pp. 89-104, 2014. https://doi.org/10.2217/nnm.12.205
48. R. Tsao, Chemistry and biochemistry of dietary polyphenols, Nutrients, vol. 2, pp. 1231-1246, 2010. https://doi.org/10.3390/nu2121231
49. M. T. Abdel Aziz, M. F. El-Asmar, A. M. Rezq, S. M. Mahfouz, M. A. Wassef, H. H. Fouad, et al., The effect of a novel curcumin derivative on pancreatic islet regeneration in experimental type-1 diabetes in rats (long term study), Diabetology & metabolic syndrome, vol. 5, pp. 1-14, 2013. https://doi.org/10.1186/1758-5996-5-75
50. Sobeh, Eman I et al. Curcumin-loaded hydroxyapatite nanocomposite as a novel biocompatible shield for male Wistar rats from γ-irradiation hazard. Chemico-bio-

logical interactions, Vol. 370, 110328, 2023. https://doi.org/10.1016/j.cbi.2022.110328
51. D.-w. Zhang, M. Fu, S.-H. Gao, and J.-L. Liu, Curcumin and diabetes: a systematic review, Evidence-Based Complementary and Alternative Medicine, vol. 2013, 2013. https://doi.org/10.1155/2013/636053
52. C. Richards-Williams, J. L. Contreras, K. H. Berecek, and E. M. Schwiebert, Extracellular ATP and zinc are co-secreted with insulin and activate multiple P2X purinergic receptor channels expressed by islet beta-cells to potentiate insulin secretion, Purinergic signalling, vol. 4, pp. 393-405, 2008. https://doi.org/10.1007/s11302-008-9126-y
53. P. Suresh Babu and K. Srinivasan, Hypolipidemic action of curcumin, the active principle of turmeric (Curcuma longa) in streptozotocin induced diabetic rats, Molecular and cellular biochemistry, 1997.
54. P. Mayes, Cholesterol synthesis, transport, and excretion in Harper's Biochemistry (Murray, RK, Mayes, PA, Granner, DK, and Rodwell, VW) pp. 253-255, Appleton & Lange, East Norwalk, 1990.
55. J. D. Bagdade, D. Porte Jr, and E. L. Bierman, Acute insulin withdrawal and the regulation of plasma triglyceride removal in diabetic subjects, Diabetes, vol. 17, pp. 127-132, 1968. https://doi.org/10.2337/diab.17.3.127
56. N. Ashokkumar, L. Pari, A. Manimekalai, and K. Selvaraju, Effect of N-benzoyl-d-phenylalanine on streptozotocin-induced changes in the lipid and lipoprotein profile in rats, Journal of pharmacy and pharmacology, vol. 57, pp. 359-366, 2005. https://doi.org/10.1211/0022357055650
57. M. Kanter, O. Coskun, A. Korkmaz, and S. Oter, Effects of Nigella sativa on oxidative stress and β-cell damage in streptozotocin-induced diabetic rats, The Anatomical Record Part A: Discoveries in Molecular, Cellular, and Evolutionary Biology: An Official Publication of the American Association of Anatomists, vol. 279, pp. 685-691, 2004. https://doi.org/10.1002/ar.a.20056
58. A. Uyar, T. Yaman, O. Kele, E. Alkan, I. Celik, and Z. Yener, Protective effects of Bryonia multiflora extract on pancreatic beta cells, liver and kidney of streptozotocin-induced diabetic rats: histopathological and immunohistochemical investigations, Indian journal of pharmaceutical education and research, vol. 51, 2017. https://doi.org/10.5530/ijper.51.3s.57
59. C. Zhang, X. Lu, Y. Tan, B. Li, X. Miao, L. Jin, et al., Diabetes-induced hepatic pathogenic damage, inflammation, oxidative stress, and insulin resistance was exacerbated in zinc deficient mouse model, PLoS One, vol. 7, p. e49257, 2012. https://doi.org/10.1371/journal.pone.0049257
60. Elbadawy, H. A., El-Dissouky, A., Hussein, S. M., El-Kewaey, S. R., Elfeky, S. A., & El-Ghannam, G. (2023). A novel terpolymer nanocomposite (carboxymethyl β-cyclodextrin-nano chitosan-glutaraldehyde) for the potential removal of a textile dye acid red 37 from water. Frontiers in Chemistry, 11. https://doi.org/10.3389/fchem.2023.1115377
61. Sobeh, E. I., El-Ghannam, G., Korany, R. M., Saleh, H. M., & Elfeky, S. A. (2023). Curcumin-loaded hydroxyapatite nanocomposite as a novel biocompatible shield for male Wistar rats from γ-irradiation hazard. Chemico-Biological Interactions, 370, 110328. https://doi.org/10.1016/j.cbi.2022.110328